Polymer Journal (2014) 46, 499–504

www.nature.com/pj

ORIGINAL ARTICLE

Biomineralization-inspired approach to the development of hybrid materials: preparation of patterned polymer/strontium carbonate thin films using thermoresponsive polymer brush matrices

Yulai Han, Tatsuya Nishimura and Takashi Kato

Thermoresponsive poly(*N*-isopropylacrylamide) (PNIPAm) brushes have been synthesized and employed as the crystallization matrices for the development of polymer/strontium carbonate hybrid materials. The use of PNIPAm brush matrices results in the formation of patterned polymer/strontium carbonate hybrid thin films in the presence of poly(acrylic acid) additives. Moreover, the conformational change in the thermoresponsive PNIPAm brush matrices induces the change in the surface morphologies of the obtained polymer/$SrCO_3$ hybrid thin films. The strategy of using stimuli-responsive polymer brush matrices is expected to be a promising method for controlling the surface morphology of two-dimensional hybrid thin film materials.
Polymer Journal (2014) **46,** 499–504; doi:10.1038/pj.2014.36; published online 21 May 2014

Keywords: biomimetic synthesis; hybrid material; poly(*N*-isopropylacrylamide); self-organization; stimuli-responsive material

INTRODUCTION

Biominerals such as nacre and bone are organic/inorganic hybrid materials with hierarchical structures and excellent mechanical properties.[1–3] The biomimetic synthesis of artificial hybrid materials via environmentally benign processes has attracted a great deal of attention for decades, aiming for the development of functional hierarchical structures under mild conditions.[4–8] Extensive studies on the biomineralization of calcium carbonate have provided insight into the development of polymer/mineral hybrid materials.[9–16] Inspired by the layered-brick-and-mortar structure of the nacre of abalone shell, two-dimensional polymer/$CaCO_3$ crystal thin films have been developed.[4,7,17–25] The synergistic effects of insoluble polymer matrices and soluble acidic polymer additives play key roles in the development of polymer/inorganic hybrid thin film materials.[4]

Recently, dynamic polymer materials such as polyrotaxanes[26–28] and stimuli-responsive polymer brushes[29] have been used to tune the morphologies of $CaCO_3$/polymer hybrids. We used carboxylated polyrotaxanes as dynamic acidic polymer additives.[25] Polymer brushes exerted great effects on $CaCO_3$ crystallization.[30,31] For example, we reported the use of poly(*N*-isopropylacrylamide) (PNIPAm) brush matrices for the formation of calcium carbonate crystal fibers.[30] PNIPAm is a thermoresponsive polymer that exhibits a lower critical solution temperature (LCST) in water at $\sim 32\,^{\circ}C$.[32] Crystallization of $CaCO_3$ at temperatures above and below the LCST of the thermoresponsive PNIPAm brush matrices induced the formation of vaterite thin films with different crystallographic orientations.[31] Polymer brushes have found applications as crystallization matrices for inorganic minerals.[30,31,33] It is of interest to control the surface patterns of the biomineralization-inspired hybrid thin films developed on polymer brush matrices.

Inorganic minerals such as hydroxyapatite,[34–36] $BaCO_3$ (see Yu *et al.*[37]) and $SrCO_3$ (see Homeijer *et al.*[38]; Sastry *et al.*[39]) have also been developed using biomimetic strategies over the past decades. Strontium carbonate, one of the representative alkaline earth carbonates with aragonitic crystal structure, has been found in coral skeletons.[40] Moreover, $SrCO_3$ has found various applications in functional optical materials[41,42] and biosensor materials for the detection of ethanol vapor.[43] $SrCO_3$ crystals with helical[44] and fibrous[45] shapes have been synthesized.

Herein, we report the synthesis and surface morphological control of polymer/$SrCO_3$ hybrid thin films using thermoresponsive PNIPAm brush matrices (Figure 1) and poly(acrylic acid) (PAA) additives.

EXPERIMENTAL PROCEDURE

Materials

PAA ($M_w = 2.0 \times 10^3$) and 2-chloropropionyl chloride (97%) were purchased from Aldrich (St Louis, MO, USA). Triethylamine (99%), (3-aminopropyl) triethoxysilane (99%) and *N*-isopropylacrylamide (NIPAm, 97%) were purchased from Tokyo Kasei (Tokyo, Japan). Copper(I) chloride (CuCl, 99.7%), dimethyl sulfoxide (99.5%), strontium chloride, ammonium

Department of Chemistry and Biotechnology, School of Engineering, University of Tokyo, Tokyo, Japan
Correspondence: Professor T Kato or Dr T Nishimura, Department of Chemistry and Biotechnology, School of Engineering, University of Tokyo, Bunkyo-ku, Tokyo 113-8656, Japan.
E-mail: kato@chiral.t.u-tokyo.ac.jp or tatsuya@chembio.t.u-tokyo.ac.jp
Received 16 March 2014; revised 6 April 2014; accepted 7 April 2014; published online 21 May 2014

carbonate and ethanol (anhydrous, 99.5%) were obtained from Wako (Tokyo, Japan). NIPAm was purified by vacuum sublimation before use.

Synthesis of PNIPAm brush matrices

PNIPAm brushes were synthesized via atom transfer radical polymerization (ATRP). First, 2-chloro-*N*-[3-(triethoxysilyl)propyl]propanamide (ATRP initiator) was synthesized by the condensation of (3-aminopropyl)triethoxysilane and 2-chloropropionyl chloride. Oxygen plasma-treated glass and silicon slides were immersed in a 10 mM solution of ATRP initiator in anhydrous ethanol for 48 h at 25 °C. The initiator-deposited substrates were dried with a stream of nitrogen. As an ATRP catalyst, tris[2-(dimethylamino) ethyl]amine (Me_6TREN) and CuCl were employed. A typical ratio of monomers and catalysts was as follows: (NIPAm)/(CuCl)/(Me_6TREN) = 1000:1:1. A solution of NIPAm (3.7 g) and dimethyl sulfoxide (5 ml) in a Schlenk tube was degassed by three freeze-pump-thaw cycles, and CuCl (3.0 mg) and Me_6TREN (8.0 mg) were added to the deoxygenated solution. The solution was subsequently transferred into a reaction vessel containing the ATRP initiator-modified substrates. After polymerization, substrates grafted with PNIPAm brushes were thoroughly washed with large quantities of methanol and deionized water.

Crystallization of $SrCO_3$

The vapor diffusion method was employed for crystallization of $SrCO_3$. Purified water for the crystallization was obtained from an Auto Pure WT100 purification system (Yamato, Tokyo, Japan; relative resistivity: maximum 1.8×10^7 Ω cm). Strontium chloride aqueous solution ($[Sr^{2+}]$ = 5 mM) containing PAA (2.5×10^{-3} wt%) was used. Crystallization was allowed to proceed in an incubator using the synthesized PNIPAm brushes as the crystallization matrices. Ammonium carbonate was placed in the incubator. Crystallization of $SrCO_3$ at temperatures above and below the LCST of the PNIPAm brushes have been carried out in this study.

Characterization

Fourier transform infrared spectra were recorded on a Jasco FT/IR-6100 spectrometer (Jasco, Tokyo, Japan). The thickness of the PNIPAm brushes was measured using a Jasco M-500 ellipsometer (Jasco) working with a helium–neon laser (λ = 632.8 nm). The thickness was also examined by tapping-mode atomic force microscopy (AFM) measurement (Bruker, Santa Barbara, CA, USA). Scanning electron microscopy (SEM) images of the hybrid samples were measured on a Hitachi S-4700 field-emission SEM (Hitachi, Tokyo, Japan) operated at 3–5 kV. Before SEM measurements, the hybrid samples were coated with a layer of platinum using a Hitachi E-1030 ion sputter coater (Hitachi). Polarizing optical microscopy images of the PNIPAm/$SrCO_3$ hybrids were obtained with an Olympus BX51 polarizing optical microscope (Olympus, Tokyo, Japan). X-ray diffraction patterns of the hybrid samples were recorded with a Rigaku SmartLab Intelligent X-ray Diffraction System (Rigaku, Tokyo, Japan) with filtered Cu Kα radiation (λ = 1.5406 Å, operating at 40 kV and 40 mA).

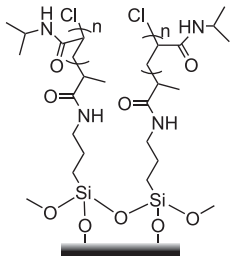

Figure 1 Structure of poly(*N*-isopropylacrylamide) (PNIPAm) brushes synthesized through atom transfer radical polymerization.

RESULTS AND DISCUSSION

The living polymerization technique allows the bottom-up synthesis of polymer brushes from initiator-deposited surfaces.[46–49] In this study, the surface-initiated ATRP technique was employed for the synthesis of PNIPAm brushes. The formation of the PNIPAm brush layer on glass and silicon substrates was confirmed by infrared measurement (Figure 2a), with characteristic absorption peaks at 3300 and 1650 cm attributable to the stretching of the amide N-H and C = O, respectively. AFM measurements performed across the scratched and unscratched boundaries show that the brush layer has a thickness of ~250 nm (Figures 2b and c).

Using the synthesized PNIPAm brushes as a matrix and PAA with a concentration of 2.5×10^{-3} wt% as a soluble additive, $SrCO_3$ has been crystallized at 20, 31 and 40 °C. The formation of crystal thin films on PNIPAm brush matrices at these temperatures is observed in the polarizing optical microscopy and SEM images (Figure 3). For thin films developed at a temperature below the LCST (20 °C) in the presence of PAA after crystallization for 8 h, the polarizing optical microscopy image shows a cross-extinction birefringence pattern because of the ordered alignment of the *c* axis (Figure 3a). In the cross-sectional SEM image of thin-film $SrCO_3$ crystals with polymer brushes (Supplementary Figure S1), the boundary between the polymer brush layer and the crystal layer is not observed, indicating that the thin film is hybrid. SEM observation shows that the hybrids formed below the LCST have dendritic surface morphologies (Figure 3b).

In contrast, crystallization at 31 °C, a temperature close to the LCST of PNIPAm brushes, resulted in the formation of crystal films with distinctly different birefringence patterns (Figure 3c). Concentric birefringence patterns are observed, and the corresponding SEM image shows that the thin film surface has periodically aligned relief patterns (Figure 3d) with a distance between two neighboring relief rings of ~5 μm.

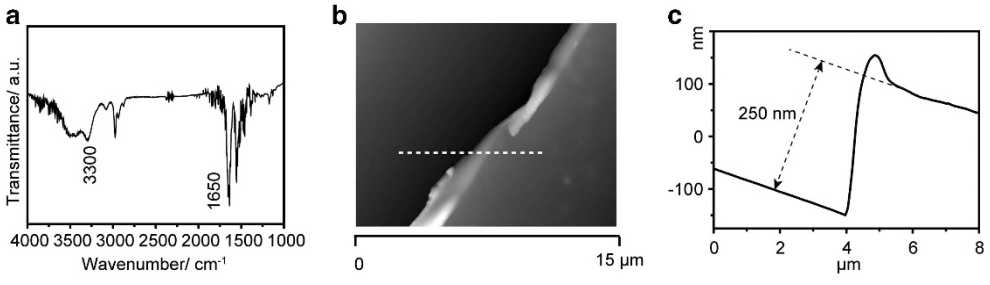

Figure 2 Surface-initiated poly(*N*-isopropylacrylamide) (PNIPAm) brush layer immobilized on a silicon substrate: (**a**) infrared (IR) spectrum of the brush layer, (**b**) cross-sectional tapping-mode atomic force microscopy (AFM) image and (**c**) cross-sectional thickness profile along the line in (**b**). A full color version of this figure is available at the *Polymer Journal* online.

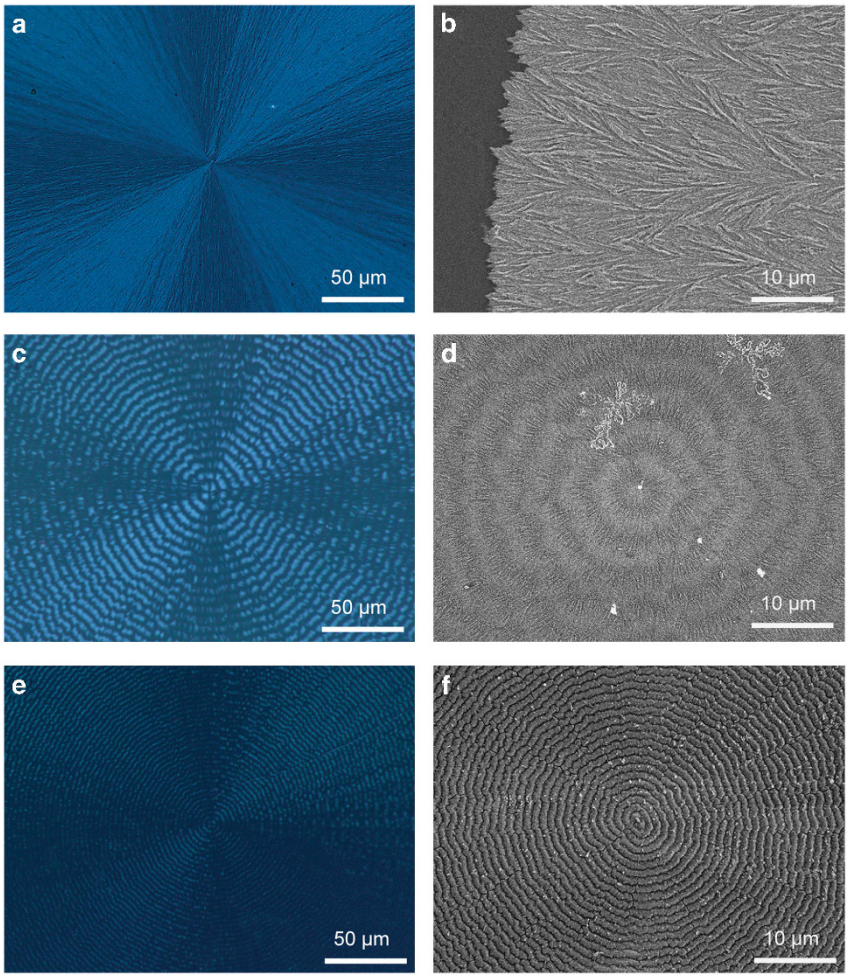

Figure 3 Crystallization of $SrCO_3$ on poly(*N*-isopropylacrylamide) (PNIPAm) brush matrices with a thickness of 250 nm in the presence of poly(acrylic acid) (PAA) with a concentration of 2.5×10^{-3} wt%. (**a**, **c**, **e**) Polarizing optical microscopy images of hybrids developed at 20 °C, 31 °C and 40 °C, respectively. (**b**, **d**, **f**) Corresponding scanning electron microscopy (SEM) images.

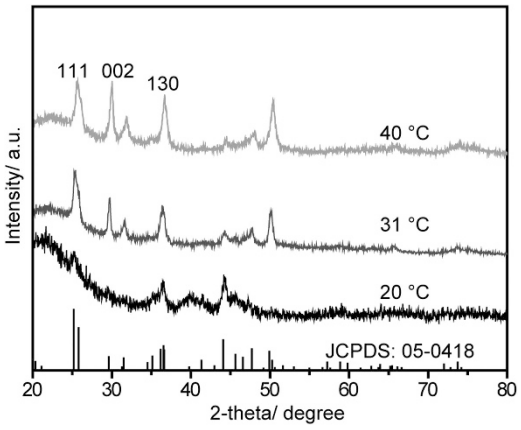

Figure 4 X-ray diffraction (XRD) patterns of crystal thin films developed at (**a**) 20 °C, (**b**) 31 °C and (**c**) 40 °C on poly(*N*-isopropylacrylamide) (PNIPAm) brush matrices with a thickness of 250 nm. A full color version of this figure is available at the *Polymer Journal* online.

Crystallization at a temperature above the LCST (40 °C) also resulted in the formation of thin films with surface relief structures (Figures 3e and f). However, a decreased periodic distance is observed compared with that on the thin films developed at 31 °C (Figures 3c and d). The approximate distance between two concentric rings is ~1 μm. X-ray diffraction measurements indicate that the crystals developed at temperatures above and below the LCST have strontium carbonate crystal structure (Figure 4) with diffraction peaks at 25.2°, 29.6° and 36.5°, corresponding to the (111), (002) and (130) planes, respectively, in strontium carbonate crystals.

AFM measurements were conducted on the thin films with relief structures that were developed on the PNIPAm matrices at 31 and 40 °C to further study the surface morphologies of the hybrid thin films (Figure 5). The concentric relief patterns on the surfaces of the hybrid films developed at 31 and 40 °C are observed on the AFM images (Figures 5a and c) that is consistent with the results obtained by SEM observation. For the thin films developed at 31 °C, the depth curve (Figure 5b) shows that the depth between the ridge and valley areas is ~50 nm. In contrast, the thin film developed at 40 °C has a relief depth of ~250 nm (Figure 5d).

Although it is difficult to fully understand the mechanism for the development of concentric relief patterns on PNIPAm brush matrices at 31 and 40 °C, it is assumed that periodic patterns formed on PNIPAm matrices are induced by a self-organization process. The concentration oscillation of ions and precursors in the polymer brushes is assumed to be essential in the formation of concentric

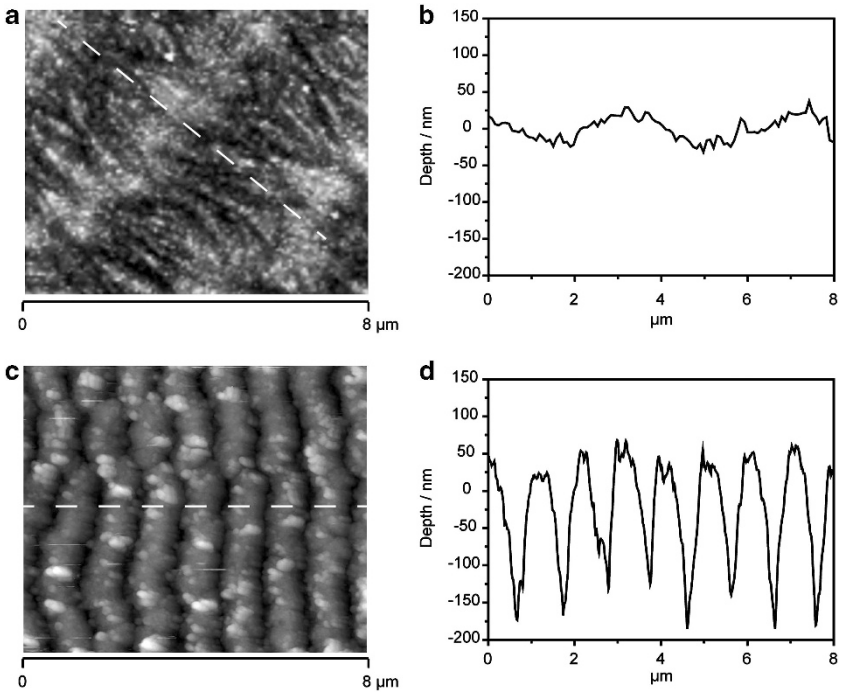

Figure 5 Atomic force microscopy (AFM) images showing the surface morphologies of the crystal thin films developed at (**a**) 31 °C and (**c**) 40 °C on poly(*N*-isopropylacrylamide) (PNIPAm) brush matrices with a thickness of 250 nm. Corresponding depth curves of the thin films developed at (**b**) 31 °C and (**d**) 40 °C with relief structures on the surfaces. A full color version of this figure is available at the *Polymer Journal* online.

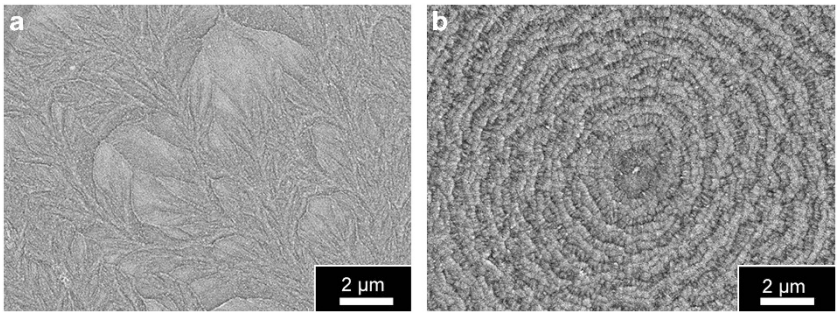

Figure 6 Crystallization of $SrCO_3$ on poly(*N*-isopropylacrylamide) (PNIPAm) brush matrices with a thickness of 25 nm in the presence of poly(acrylic acid) (PAA) with a concentration of 2.5×10^{-3} wt%. Scanning electron microscopy (SEM) images of the hybrids developed at temperatures (**a**) below (20 °C) and (**b**) above (40 °C) the lower critical solution temperature (LCST).

patterns, as has been observed for crystallization in gel media.[21,50–53] In the presence of PAA additives, crystallization of $SrCO_3$ is a reaction–diffusion system. For the crystallization of $SrCO_3$, Gower and colleagues[38] reported that PAA additives favor the formation of amorphous precursors or polymer-induced liquid precursor phases. These precursor phases could diffuse onto the surface of the PNIPAm brush matrices and lead to crystal nucleation and growth. The diffusion and consumption of the precursor phases induces the fluctuations in the concentration of the amorphous precursor phase. It is assumed that the concentration fluctuation together with the effect of polymer brush matrices results in the formation of concentric relief patterns.

To examine the role of polymer brush thickness, PNIPAm brush matrices with a thickness of ~25 nm were also employed as crystallization matrices. It is noteworthy that $SrCO_3$ crystal thin films developed on PNIPAm brush matrices with a thickness of 25 nm at temperatures above and below the LCST also show distinctly different surface morphologies (Figure 6). Crystallization at a temperature below the LCST (20 °C) results in the formation of crystals with dendritic patterns (Figure 6a), whereas thin films developed at a temperature above the LCST (40 °C) show concentric patterns (Figure 6b). Further characterization by AFM shows that the distance between two neighboring rings is ~2 μm with a relief depth of ~100 nm (Figures 7a and b). This relief depth is smaller than that for thin films developed using PNIPAm brush matrices with a thickness of 250 nm. The thickness of PNIPAm brushes is assumed to be influential on their aggregation states that probably affects crystallization and ion diffusion behavior.

The use of PNIPAm brush matrices at temperatures above and below the LCST led to the development of $SrCO_3$/PNIPAm hybrid thin films with distinct surface morphologies. Although temperature is an important factor that probably influences crystal nucleation and growth, the surface morphology changes of the thin films developed on PNIPAm brush matrices are assumed to be attributable to the

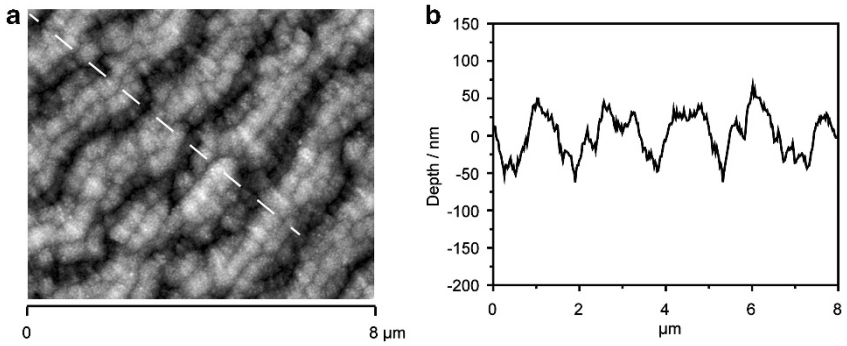

Figure 7 (**a**) Atomic force microscopy (AFM) image and (**b**) corresponding depth curve of the thin film with surface relief structures developed on a poly(*N*-isopropylacrylamide) (PNIPAm) brush matrix with a thickness of 25 nm at a temperature above (40 °C) the lower critical solution temperature (LCST). A full color version of this figure is available at the *Polymer Journal* online.

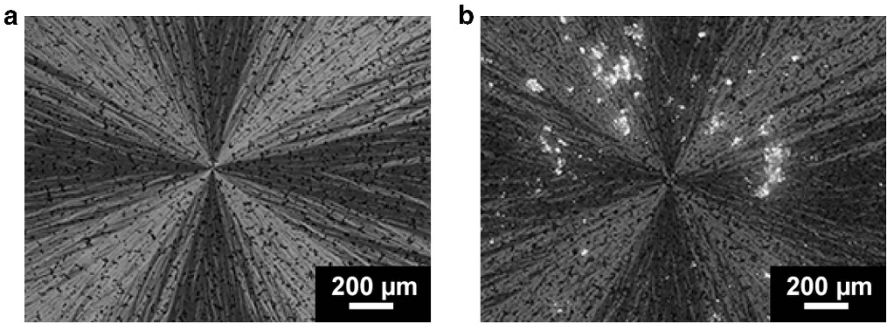

Figure 8 Crystallization of $SrCO_3$ on chitosan matrices in the presence of poly(acrylic acid) (PAA) with a concentration of 2.5×10^{-3} wt%. Polarizing optical microscopy images of hybrids developed at (**a**) 20 °C and (**b**) 40 °C. A full color version of this figure is available at the *Polymer Journal* online.

conformational changes of the PNIPAm chains at temperatures above and below the LCST. To examine the matrix effect of the thermo-responsive PNIPAm brushes, chitosan was employed as a nonstimuli-responsive matrix. Spin-coated chitosan matrices thermally annealed at 110 °C for 30 min were used for the crystallization of $SrCO_3$. Thin films developed at 20 and 40 °C on chitosan matrices in the presence of PAA additives show similar birefringence patterns (Figure 8). In comparison with chitosan, it is known that the chains in PNIPAm brushes show a dramatic conformational change from a stretched state at temperatures below the LCST to an aggregated state at temperatures above the LCST. The structural variation of polymer brush matrices may change ionic diffusion behaviors. For instance, Huang *et al.*[54] studied the interactions between ions and polyethylene membrane grafted with a PNIPAm layer. They showed a significant change in the Zeta potential of the membrane across the LCST of PNIPAm. In the present study, it is assumed that for the PNIPAm brush in the crystallization system, the change in the Zeta potential influences its affinity for ions or amorphous precursors, thus resulting in different crystallization behavior at temperatures above and below the LCST. Mano and colleagues[55] reported the formation of apatite on PNIPAm-grafted poly(L-lactic acid) matrices only at temperatures above the LCST, indicating the influence of the PNIPAm conformational structure on the crystallization of apatite.

CONCLUSION

We have found that thermoresponsive PNIPAm brushes are effective matrices for the crystallization of $SrCO_3$. PNIPAm/$SrCO_3$ hybrid thin films with different surface morphologies have been synthesized by utilizing the thermoresponsiveness of PNIPAm brush matrices in the presence of PAA additives. This approach of using stimuli-responsive polymer brush matrices for the tuning of the surface morphology of hybrid thin films is expected to contribute to new developments in materials design.

ACKNOWLEDGEMENTS

This work was supported by a Grant-in-Aid for Scientific Research (no. 22107003) on the Innovative Areas, 'Fusion Materials: Creative Development of Materials and Exploration of Their Function through Molecular Control' (area no. 2206) from the Ministry of Education, Culture, Sports, Science and Technology (MEXT).

1 Mann, S. *Biomineralization: Principles and Concepts in Bioinorganic Materials Chemistry* (Oxford University Press, New York, 2001).
2 Baeuerlein, E., Behrens, P. & Epple, M. *Handbook of Biomineralization* (Wiley-VCH, Weinheim, 2007).
3 Dove, P. M., De Yoreo, J. & Weiner, S. *Biomineralization* (Mineralogical Society of America, Washington, DC, 2003).
4 Kato, T., Sakamoto, T. & Nishimura, T. Macromolecular templating for the formation of inorganic-organic hybrid structures. *MRS Bull.* **35,** 127–132 (2010).
5 Nudelman, F. & Sommerdijk, N. A. J. M. Biomineralization as an inspiration for materials chemistry. *Angew. Chem. Int. Ed.* **51,** 6582–6596 (2012).
6 Sugawara-Narutaki, A. Bio-inspired synthesis of polymer-inorganic nanocomposite materials in mild aqueous systems. *Polym. J.* **45,** 269–276 (2013).
7 Kato, T., Sugawara, A. & Hosoda, N. Calcium carbonate-organic hybrid materials. *Adv. Mater.* **14,** 869–877 (2002).
8 Yao, H. B., Fang, H. Y., Wang, X. H. & Yu, S. H. Hierarchical assembly of micro-/nano-building blocks: bio-inspired rigid structural functional materials. *Chem. Soc. Rev.* **40,** 3764–3785 (2011).
9 Oaki, Y., Kajiyama, S., Nishimura, T., Imai, H. & Kato, T. Nanosegregated amorphous composites of calcium carbonate and an organic polymer. *Adv. Mater.* **20,** 3633–3637 (2008).

10 Kim, Y. Y., Ganesan, K., Yang, P. C., Kulak, A. N., Borukhin, S., Pechook, S., Ribeiro, L., Kroger, R., Eichhorn, S. J., Armes, S. P., Pokroy, B. & Meldrum, F. C. An artificial biomineral formed by incorporation of copolymer micelles in calcite crystals. *Nat. Mater.* **10,** 890–896 (2011).
11 Tanaka, Y. & Naka, K. Synthesis of calcium carbonate particles with carboxylic-terminated hyperbranched poly(amidoamine) and their surface modification. *Polym. J.* **44,** 586–593 (2012).
12 Yamamoto, Y., Nishimura, T., Saito, T. & Kato, T. $CaCO_3$/chitin-whisker hybrids: formation of $CaCO_3$ crystals in chitin-based liquid-crystalline suspension. *Polym. J.* **42,** 583–586 (2010).
13 Nishimura, T., Ito, T., Yamamoto, Y., Yoshio, M. & Kato, T. Macroscopically ordered polymer/$CaCO_3$ hybrids prepared by using a liquid-crystalline template. *Angew. Chem. Int. Ed.* **47,** 2800–2803 (2008).
14 Saito, T., Oaki, Y., Nishimura, T., Isogai, A. & Kato, T. Bioinspired stiff and flexible composites of nanocellulose-reinforced amorphous $CaCO_3$. *Mater. Horiz* **1,** 321–325 (2014).
15 Oaki, Y., Adachi, R. & Imai, H. Self-organization of hollow-cone carbonate crystals through molecular control with an acid organic polymer. *Polym. J.* **44,** 612–619 (2012).
16 Cölfen, H. & Mann, S. Higher-order organization by mesoscale self-assembly and transformation of hybrid nanostructures. *Angew. Chem. Int. Ed.* **42,** 2350–2365 (2003).
17 Kato, T., Suzuki, T., Amamiya, T., Irie, T., Komiyama, M. & Yui, H. Effects of macromolecules on the crystallization of $CaCO_3$ the formation of organic/inorganic composites. *Supramol. Sci.* **5,** 411–415 (1998).
18 Kato, T. Polymer/calcium carbonate layered thin-film composites. *Adv. Mater.* **12,** 1543–1546 (2000).
19 Kato, T., Suzuki, T. & Irie, T. Layered thin-film composite consisting of polymers and calcium carbonate: a novel organic/inorganic material with an organized structure. *Chem. Lett.* **29,** 186–187 (2000).
20 Sugawara, A., Oichi, A., Suzuki, H., Shigesato, Y., Kogure, T. & Kato, T. Assembled structures of nanocrystals in polymer/calcium carbonate thin-film composites formed by the cooperation of chitosan and poly(aspartate). *J. Polym. Sci., A Polym. Chem.* **44,** 5153–5160 (2006).
21 Sakamoto, T., Oichi, A., Oaki, Y., Nishimura, T., Sugawara, A. & Kato, T. Three-dimensional relief structures of $CaCO_3$ crystal assemblies formed by spontaneous two-step crystal growth on a polymer thin film. *Cryst. Growth Des.* **9,** 622–625 (2009).
22 Sakamoto, T., Nishimura, Y., Nishimura, T. & Kato, T. Photoimaging of self-organized $CaCO_3$/polymer hybrid films by formation of regular relief and flat surface morphologies. *Angew. Chem. Int. Ed.* **50,** 5856–5859 (2011).
23 Kajiyama, S., Nishimura, T., Sakamoto, T. & Kato, T. Aragonite nanorods in calcium carbonate/polymer hybrids formed through self-organization processes from amorphous calcium carbonate solution. *Small* **10,** 1634–1641 (2014).
24 Zhu, F. J., Nishimura, T., Sakamoto, T., Tomono, H., Nada, H., Okumura, Y., Kikuchi, H. & Kato, T. Tuning the stability of $CaCO_3$ crystals with magnesium ions for the formation of aragonite thin films on organic polymer templates. *Chem.-Asian J.* **8,** 3002–3009 (2013).
25 Zhu, F., Nishimura, T., Eimura, H. & Kato, T. Supramolecular effects on formation of $CaCO_3$ thin films on a polymer matrix. *CrystEngComm* **16,** 1496–1501 (2014).
26 Harada, A., Takashima, Y. & Yamaguchi, H. Cyclodextrin-based supramolecular polymers. *Chem. Soc. Rev.* **38,** 875–882 (2009).
27 Koyama, Y., Suzuki, Y., Asakawa, T., Kihara, N., Nakazono, K. & Takata, T. Polymer architectures assisted by dynamic covalent bonds: synthesis and properties of boronate-functionalized polyrotaxane and graft polyrotaxane. *Polym. J.* **44,** 30–37 (2012).
28 Ito, K. Novel entropic elasticity of polymeric materials: why is slide-ring gel so soft? *Polym. J.* **44,** 38–41 (2012).
29 Yamago, S., Yahata, Y., Nakanishi, K., Konishi, S., Kayahara, E., Nomura, A., Goto, A. & Tsujii, Y. Synthesis of concentrated polymer brushes via surface-initiated organotellurium-mediated living radical polymerization. *Macromolecules* **46,** 6777–6785 (2013).
30 Kumar, S., Ito, T., Yanagihara, Y., Oaki, Y., Nishimura, T. & Kato, T. Crystallization of unidirectionally oriented fibrous calcium carbonate on thermo-responsive polymer brush matrices. *CrystEngComm* **12,** 2021–2024 (2010).
31 Han, Y., Nishimura, T. & Kato, T. Morphology tuning in the formation of vaterite crystal thin films with thermo-responsive poly(*N*-isopropylacrylamide) brush matrices. *CrystEngComm* **16,** 3540–3547 (2014).
32 Schild, H. G. Poly (*N*-Isopropylacrylamide) - experiment, theory and application. *Prog. Polym. Sci.* **17,** 163–249 (1992).
33 Tugulu, S., Harms, M., Fricke, M., Volkmer, D. & Klok, H. A. Polymer brushes as ionotropic matrices for the directed fabrication of microstructured calcite thin films. *Angew. Chem. Int. Ed.* **45,** 7458–7461 (2006).
34 Ohtsuki, C., Kamitakahara, M. & Miyazaki, T. Coating bone-like apatite onto organic substrates using solutions mimicking body fluid. *J. Tissue Eng. Regen. Med.* **1,** 33–38 (2007).
35 Nishimura, T., Mai, H., Oaki, Y., Sakamoto, T. & Kato, T. Preparation of thin-film hydroxyapatite/polymer hybrids. *Chem. Lett.* **40,** 458–460 (2011).
36 Furuichi, K., Oaki, Y. & Imai, H. Preparation of nanotextured and nanoribrous hydroxyapatite through dicalcium phosphate with gelatin. *Chem. Mater.* **18,** 229–234 (2006).
37 Yu, S. H., Cölfen, H., Tauer, K. & Antonietti, M. Tectonic arrangement of $BaCO_3$ nanocrystals into helices induced by a racemic block copolymer. *Nat. Mater.* **4,** 51–55 (2005).
38 Homeijer, S. J., Barrett, R. A. & Gower, L. B. Polymer-induced liquid-precursor (PILP) process in the non-calcium based systems of barium and strontium carbonate. *Cryst. Growth Des.* **10,** 1040–1052 (2010).
39 Sastry, M., Kumar, A., Damle, C., Sainkar, S. R., Bhagwat, M. & Ramaswamy, V. Crystallization of $SrCO_3$ within thermally evaporated fatty acid films: unusual morphology of crystal aggregates. *CrystEngComm* **3,** 81–83 (2001).
40 Greegor, R. B., Pingitore, N. E. & Lytle, F. W. Strontianite in coral skeletal aragonite. *Science* **275,** 1452–1454 (1997).
41 Tagaya, A., Ohkita, H., Mukoh, M., Sakaguchi, R. & Koike, Y. Compensation of the birefringence of a polymer by a birefringent crystal. *Science* **301,** 812–814 (2003).
42 Tagaya, A. & Koike, Y. Compensation and control of the birefringence of polymers for photonics. *Polym. J.* **44,** 306–314 (2012).
43 Shi, J. J., Li, J. J., Zhu, Y. F., Wei, F. & Zhang, X. R. Nanosized $SrCO_3$-based chemiluminescence sensor for ethanol. *Anal. Chim. Acta* **466,** 69–78 (2002).
44 Terada, T., Yamabi, S. & Imai, H. Formation process of sheets and helical forms consisting of strontium carbonate fibrous crystals with silicate. *J. Cryst. Growth* **253,** 435–444 (2003).
45 Balz, M., Therese, H. A., Kappl, M., Nasdala, L., Hofmeister, W., Butt, H. J. & Tremel, W. Morphosynthesis of strontianite nanowires using polyacrylate templates tethered onto self-assembled monolayers. *Langmuir* **21,** 3981–3986 (2005).
46 Kato, M., Kamigaito, M., Sawamoto, M. & Higashimura, T. Polymerization of methyl methacrylate with the carbon tetrachloride dichlorotris(triphenylphosphine) ruthenium(II) methylaluminum bis(2,6-di-tert-butylphenoxide) initiating system: possibility of living radical polymerization. *Macromolecules* **28,** 1721–1723 (1995).
47 Matyjaszewski, K. & Xia, J. H. Atom transfer radical polymerization. *Chem. Rev.* **101,** 2921–2990 (2001).
48 Ouchi, M., Yoda, H., Terashima, T. & Sawamoto, M. Aqueous metal-catalyzed living radical polymerization: highly active water-assisted catalysis. *Polym. J.* **44,** 51–58 (2012).
49 Sakurai, S., Watanabe, H. & Takahara, A. Preparation and characterization of looped polydimethylsiloxane brushes. *Polym. J.* **46,** 117–122 (2014).
50 Sugawara, A., Ishii, T. & Kato, T. Self-organized calcium carbonate with regular surface-relief structures. *Angew. Chem. Int. Ed.* **42,** 5299–5303 (2003).
51 Cartwright, J. H. E., Garcia-Ruiz, J. M. & Villacampa, A. I. Pattern formation in crystal growth: Liesegang rings. *Comput. Phys. Commun.* **121,** 411–413 (1999).
52 Klajn, R., Fialkowski, M., Bensemann, I. T., Bitner, A., Campbell, C. J., Bishop, K., Smoukov, S. & Grzybowski, B. A. Multicolour micropatterning of thin films of dry gels. *Nat. Mater.* **3,** 729–735 (2004).
53 Smoukov, S. K., Bitner, A., Campbell, C. J., Kandere-Grzybowska, K. & Grzybowski, B. A. Nano- and microscopic surface wrinkles of linearly increasing heights prepared by periodic precipitation. *J. Am. Chem. Soc.* **127,** 17803–17807 (2005).
54 Huang, J., Wang, X. L., Qi, W. S. & Yu, X. H. Temperature sensitivity and electrokinetic behavior of a *N*-isopropylacrylamide grafted microporous polyethylene membrane. *Desalination* **146,** 345–351 (2002).
55 Shi, J., Alves, N. M. & Mano, J. F. Thermally responsive biomineralization on biodegradable substrates. *Adv. Funct. Mater.* **17,** 3312–3318 (2007).

Supplementary Information accompanies the paper on Polymer Journal website (http://www.nature.com/pj)